Microchimica Acta (2020) 187:348
https://doi.org/10.1007/s00604-020-04320-9

ORIGINAL PAPER

# Oriented boronate affinity–imprinted inverse opal hydrogel for glycoprotein assay via colorimetry

Huan Wang[1,2] · Jie Wang[2,3] · Yuetong Wang[2] · Yuqin Liu[2] · Rui Liu[4] · Xuelin Wang[5] · Hui Tan[1,6] · Tianfu Wang[1] · Tiantian Kong[1]

Received: 3 November 2019 / Accepted: 13 May 2020


## Abstract

A biomimetic antibody is described for colorimetric determination of glycoprotein, and horseradish peroxidase (HRP) is used as model analyte. Use is made of oriented surface imprinted inverse opal hydrogel particles functionalized with phenylboronic acid. The inverse opal hydrogel particles were negatively replicated from silica colloidal crystal beads (SCCBs), so that they were endowed with larger specific surface area than the bulk structure. Benefit from that, there were abundant surface molecularly imprinting sites in the hydrogel particles. Because the imprinting sites match the structure of the template molecules, they can recognize HRP with high selectivity and sensitivity. The recognized glycoprotein was bonded with the phenylboronic acid within the sites. The bonded HRP was determined by colorimetry of 3, 3′, 5, 5′-tetramethylbenzidine (TMB) single-component solution at 450 nm, and it shows a 16.03 imprinting factor under optimized conditions. Alpha-fetoprotein (AFP) was also investigated and demostrated the value of this strategy in practical applications. The results show that the absorbance increases linearly in the 1–50 ng $mL^{-1}$ AFP concentration range and has a 1.32 ng $mL^{-1}$ detection limit. The assay of human serum was realized by the standard addition method. This strategy is promising to open new horizons for glycoprotein assay.

**Keywords** Oriented surface molecularly imprinting · Colloidal crystal · Microfluidics · Hydrogel · Large specific surface area · Biomimetic antibody · Label-free detection · ELISA · Optical biosensor

## Introduction

Glycoproteins, as a series of proteins with glycosylation site(s), exist widely in many kinds of beings and play key roles in various biological processes. Generally, the concentration of every kind of glycoproteins in body is relatively constant. However, when the biological processes of the body have some problems, some kinds of glycoproteins would show significant concentration changes. Thus, the glycoproteins are used as disease biomarkers

**Electronic supplementary material** The online version of this article (https://doi.org/10.1007/s00604-020-04320-9) contains supplementary material, which is available to authorized users.

✉ Huan Wang

✉ Hui Tan
huitan@email.szu.edu.cn

✉ Tianfu Wang
tfwang@szu.edu.cn

✉ Tiantian Kong
ttkong@szu.edu.cn

[1] Department of Biomedical Engineering, The First Affiliated Hospital, Shenzhen University, Shenzhen 518035, China

[2] State Key Laboratory of Bioelectronics, School of Biological Science and Medical Engineering, Southeast University, Nanjing 210096, China

[3] College of Engineering, Nanjing Agricultural University, Nanjing 210031, China

[4] Department of Genetic Engineering, College of Natural Science, University of Suwon, Hwaseong 445-743, Kyunggi-Do, Republic of Korea

[5] Ulink College of Suzhou Industrial Park, Suzhou 215007, China

[6] Department of Neurosurgery, The First Affiliated Hospital, Shenzhen University, Shenzhen 518035, China

Published online: 27 May 2020

for clinical diagnostics. There are many attempts that have been developed for the glycoprotein determination [1–6]. Although these methods have displayed high sensitivity and specificity, most of them often suffered from the poor stability, high-consuming, and the expensive equipment. Boronate affinity–based molecularly imprinted materials have been proven as an efficient tool for the glycoprotein recognition in recent decades [7–9]. Molecularly imprinted polymers (MIP) are a kind of materials with special recognition sites for binding with the imprinted molecules as biomimetic antibody. They have been used in various applications such as sensing, separation, catalysis, and drug delivery [10–14]. Boronic acid–based materials have superb characteristics on reversible binding with *cis*-diol-containing molecules, for instance sugars and glycoproteins [15–17]. Thus, boronate affinity–based molecularly imprinted materials are promising for glycoproteins recognition with high specificity, good stability, and low cost. Even with these merits, most of the boronate affinity–based molecularly imprinted materials are suffering from the limited efficiency and sensitivity. These are because of the bulk structure resulted small quantities of recognition sites [18]. Therefore, a stable, specific, sensitive, and inexpensive approach for the determination of glycoproteins is still anticipated.

In this study, we present a novel oriented boronate affinity–imprinted inverse opal particles for the desired determination. The particles are fabricated by infusing oriented boronate affinity–imprinted materials into the inverse opal structures. Oriented boronate affinity–imprinted materials, as a kind of boronate affinity MIP whose recognition sites only exist on the surface, can assay glycoproteins with fast responsiveness [18–20]. Inverse opals [21–25] are a kind of structural materials featured in the three-dimensional (3D) ordered macropores which are negatively replicated from colloidal crystal templates [26–28]. Herein, we employed silica colloidal crystal beads (SCCBs) generated from microfluidic as templates [29–32]. This unique structure endows them with much larger specific surface area than bulk materials [33–36]. As the imprinted sites of molecules are oriented on the surface of the inverse opal particles, the particles can provide more imprinted sites than bulk structure and results in higher sensitivity. Thus, the combination of oriented boronate affinity–imprinted materials and inverse opals endows the particles with advantages of specificity, efficiency, and sensitivity for glycoprotein determination. It is the first time to combine these two factors together to construct oriented boronate affinity–imprinted inverse opal particles for determination. This method is not only stable and low cost but also specific and sensitive to the target glycoprotein. Therefore, this new approach is promising to open new horizons in construction of glycoprotein assay platform.

## Experimental methods

### Materials

The silica nanoparticles used in this study were homemade. 3-acrylamidophenylboronic acid (APBA), acrylamide (AAm), *N,N′*-Methylenebis(acrylamide) (Bis), 2-hydroxy-2-methylpropiophenone (HMPP), 3-aminopropyl triethoxysilane (APTES), and transferrin (TRF, glycoprotein with 2 glycosylation sites) were obtained from Sigma-Aldrich (https://www.sigmaaldrich.com). Horseradish peroxidase (HRP, glycoprotein with 9 glycosylation sites), albumin from bovine serum (BSA, non-plycoprotin), hydrofluoric acid (HF), and 4-formylphenylboronic acid (FPBA) were bought from Aladdin Industrial Co., Ltd. (Shanghai, China) (http://www.aladdine.com). 3,3,5′,5′-Tetramethylbenzidine dihydrochloride (TMB) single-component substrate solution (containing TMB and hydrogen peroxide ($H_2O_2$) simultaneously) was obtained from Beyotime Biotechnology Co., Ltd. (Shanghai, China) (https://www.beyotime.com). Sodium hydroxide (NaOH), tris base, glacial acetic acid (HAc), hydrochloric acid (HCl), glucose, and ethanol were purchased from Sinopharm Chemical Reagent (Shanghai, China) (https://www.reagent.com.cn). Alpha-fetoprotein (AFP, glycoprotein with 11 glycosylation sites) and HRP-labeled anti-AFP were obtained from Biocell Co., Ltd. (Zhengzhou, China) (www.cnbiocell.com). Hypermer 2296 surfactant (nonionic surfactant ethoxylated ester) was purchased from Croda International Plc (https://www.croda.com). Sodium cyanoborohydride was purchased from Macklin Biochemical Co., Ltd. (Shanghai, China) (www.macklin.cn). Other reagents were analytical grade or higher, and all the reagents were used as received. Water used in all experiments was purified using a Milli-Q Plus 185 water purification system (Millipore, Bedford, MA) with resistivity higher than 18 MΩ cm.

### Fabrication of silica colloidal crystal beads (SCCBs)

The silica colloidal crystal particles were prepared by the droplet templates generated from gravity-driven microfluidics with a single emulsion glass microfluidic chip. The monodispersed silica nanoparticles solution were tuned to 20 wt% (2.5 mL) and used as the inner phase, and *n*-hexadecane containing 1 wt% hypermer 2296 surfactant (20 mL) was used as outer phase. The flow rates of the inner phase and outer phase were 1 mL/h and 6 mL/h, respectively. When the two fluids met in the microfluidic channel, the outer phase cut the inner phase into droplets, and the droplets were collected by a hydrophobic box containing *n*-hexadecane with 1 wt% hypermer 2296. Then the box was heated by a heating stage at 70 °C for 2 days. Finally, the dried particles were calcined at 800 °C for 3 h. The microstructures of the particles

were characterized by a scanning electron microscopy (SEM, Hitachi, S-300 N).

## Modification of silica colloidal crystal beads (SCCBs)

The silica colloidal crystal particles (25 μL for each operation) were treated to expose hydroxyl by immersing in 200 μL 0.1 mol·$L^{-1}$ NaOH solution at room temperature, shaken slightly for 1 h firstly. After being washed with deionized (DI) water at least 3 times, the particles were dried by a drying oven. Then the dried particles were immersed in 200 μL solution of 10% APTES in ethanol, shaken gently overnight to modify amino groups. Subsequently, the particles were washed by ethanol 5 times. 10 mg·$mL^{-1}$ FPBA in ethanol (200 μL) was used to form Schiff base to modify boronate acid groups by incubating the particles and shaken slightly for 12 h after drying. Next, the particles were treated with additional 200 μL 10 mg $mL^{-1}$ sodium cyanoborohydride and shaken gently for 24 h to reduce the imine. Finally, the particles were washed by ethanol 5 times and dried.

## Characterization of the modified silica colloidal crystal beads (SCCBs)

The 200 ng $mL^{-1}$ HRP solution dissolved in Tris-HCl buffer (50 mM, pH 8.5) was used to incubate the unmodified, amino-modified, and FPBA-modified particles, respectively, for 2 h. Each type of particles was 5 μL and treated with 200-μL HRP solution. Then the particles were washed by the Tris-HCl buffer (50 mM, pH 8.5, with 0.05% Tween 20) 5 times. All of the particles were treated with 200 μL TMB single-component substrate, respectively. Ten minutes later, 100 μL 2 M $H_2SO_4$ was added into the solution in several to stop the enzyme reaction, and the absorbance of the mixed solution were measured at 450 nm.

## The effect of pH on the binding of horseradish peroxidase (HRP) with the modified silica colloidal crystal beads (SCCBs)

1 mL 200 ng·$mL^{-1}$ HRP solution dissolved in 0.1% HAc (pH 3.5), 50 mM phosphate-buffered solution with different pH (4.7, 6.0, and 7.4), or 50 mM Tris-HCl buffer (pH 8.5) was used to incubate the FPBA-modified particles (5 μL for each group) for 2 h. Then the particles were washed by the corresponding buffer (with 0.05% Tween 20) 5 times. Next, the particles were washed by Tris-HCl buffer (50 mM, pH 8.5, with 0.05% Tween 20) 5 times. All of the particles were treated with 200 μL TMB single-component substrate, respectively. After 10 min, 100 μL 2 M $H_2SO_4$ was added into the solution in several to stop the enzyme reaction, and the absorbance of the mixed solution were measured at 450 nm.

## Preparation of the horseradish peroxidase (HRP)–imprinted molecularly imprinted polymer (MIP) particles

The FPBA-modified silica colloidal crystal particles (25 μL for each operation) were incubated in 1 mL 10 μg $mL^{-1}$ HRP dissolved in Tris-HCl buffer (50 mM, pH 8.5) 2 h firstly. Then the particles were washed by Tris-HCl buffer (50 mM, pH 8.5, with 0.05% Tween 20) 5 times. Next, 100 μL 100 μg $mL^{-1}$ APBA solution was used to bind with the HRP for 3 h. After washed by Tris-HCl buffer (50 mM, pH 8.5, with 0.05% Tween 20), the residual APBA were removed. 100 μL AA/Bis pregel solution dissolved in Tris-HCl buffer (50 mM, pH 8.5) containing 1% HMPP was used to immerse the particles and slightly shaken for 3 h. Subsequently, the particles with the pregel solution exposed to 365 nm UV light for 10 s and the hybrid particles were obtained. Finally, the hybrid particles were etched by HF solution. Because all the polymerized APBA were bonded with HRP firstly, they were only existed in the imprinted sites of HRP of the final material. NIP (non-molecularly imprinted polymer) was prepared with the same procedures except that the HRP solutions were replaced by Tris-HCl buffer (50 mM, pH 8.5). The optical images were observed by a stereomicroscope (Nanjing Jiangnan Novel Optics Co., Ltd.) with a CCD camera (Media Cybernetics EvolutionMP 5.0). The microstructures of the particles were characterized by a scanning electron microscopy (SEM, Hitachi, S-300 N).

## Optimizing the binding pH in assay process

The MIP particles (5 μL for each group) were incubated in 200 μL 10 μg $mL^{-1}$ HRP dissolved in 0.1% HAc (pH 3.5), 50 mM phosphate-buffered solution with different pH (5.0, 6.0, and 7.4), or 50 mM Tris-HCl buffer (pH 8.5) for 2 h firstly. Then the particles were washed by the corresponding buffer (with 0.05% Tween 20) 5 times and Tris-HCl buffer (50 mM, pH 8.5, with 0.05% Tween 20) 5 times successively. Next, all of the particles were treated with 200 μL TMB single-component substrate, respectively. After 30 min, 100 μL 2 M $H_2SO_4$ was added into the solution in several to stop the enzyme reaction, and the absorbance of the mixed solution were measured at 450 nm.

## The tolerance to interference of the molecularly imprinted polymer (MIP) particles

The samples were 10 μg $mL^{-1}$ HRP dissolved in Tris-HCl buffer (50 mM, pH 8.5). Glucose, BSA, and TRF were used as interfering substance with a high concentration of 10 mg·$mL^{-1}$, respectively. The MIP particles (5 μL for each group) were incubated in different samples (200 μL) for 2 h. Then the particles were washed by Tris-HCl buffer (50 mM, pH 8.5,

with 0.05% Tween 20) 5 times. Next, all of the particles were treated with 200 μL TMB single-component substrate, respectively. Thirty minutes later, 100 μL 2 M $H_2SO_4$ was added into the solution in several to stop the enzyme reaction, and the absorbance of the mixed solution were measured at 450 nm.

### Binding equilibrium of the molecularly imprinted polymer (MIP) particles

The sample was 100 μg·mL$^{-1}$ HRP dissolved in Tris-HCl buffer (50 mM, pH 8.5). The MIP particles (5 μL for each group) were incubated in the samples (200 μL) for different time. Then the particles were washed by Tris-HCl buffer (50 mM, pH 8.5, with 0.05% Tween 20) 5 times. Next, all of the particles were treated with 200 μL TMB single-component substrate, respectively. Thirty minutes later, 100 μL 2 M $H_2SO_4$ was added into the solution in several to stop the enzyme reaction, and the absorbance of the mixed solution were measured at 450 nm.

### Binding isotherm of the molecularly imprinted polymer (MIP) particles

The MIP particles (5 μL for each group) were incubated in the HRP solution (200 μL) with different concentration in Tris-HCl buffer (50 mM, pH 8.5) for 2 h firstly. Then the particles were washed by Tris-HCl buffer (50 mM, pH 8.5, with 0.05% Tween 20) 5 times. Next, all of the particles were treated with 200 μL TMB single-component substrate, respectively. Thirty minutes later, 100 μL 2 M $H_2SO_4$ was added into the solution in several to stop the enzyme reaction, and the absorbance of the mixed solution were measured at 450 nm.

### Binding isotherm of the alpha-fetoprotein-molecularly imprinted polymer (AFP-MIP) particles

The AFP-MIP particles were prepared using the same procedure as the HRP-MIP particles at the optimized conditions, except that the HRP was replaced by AFP. For the binding isotherm, the MIP particles (5 μL for each group) were incubated in the AFP solution (200 μL) with different concentration in Tris-HCl buffer (50 mM, pH 8.5) for 2 h firstly. After being washed by Tris-HCl buffer (50 mM, pH 8.5, with 0.05% Tween 20) 5 times, 10 mg mL$^{-1}$ BSA solution (200 μL) dissolved in Tris-HCl buffer (50 mM, pH 8.5) was added and incubated for 30 min. The BSA solution was used for reducing the nonspecific adsorption. Then the solution was replaced by 1 μg·mL$^{-1}$ HRP-labeled anti-AFP solution (200 μL) dissolved in phosphate-buffered solution (10 mM, pH 7.4) and incubated for 30 min. Subsequently, the particles were washed by phosphate-buffered solution (10 mM, pH 7.4, with 0.05% Tween 20) 5 times. Next, all of the particles were treated with 200 μL TMB single-component substrate, respectively. Thirty minutes later, 100 μL 2 M $H_2SO_4$ was added into the solution in several to stop the enzyme reaction, and the absorbance of the mixed solution were measured at 450 nm.

## Results and discussion

As a proof of concept, the horse radish peroxidase (HRP) was used as target glycoprotein to construct oriented surface boronate affinity–imprinted inverse opal particles. SCCBs were employed to be the templates for constructing inverse opal hydrogel and the substrate for the immobilization of target glycoprotein. Figure 1 and Fig. S1 show the principle and procedure of the process. Firstly, the hydrophilic SCCBs were treated by 3-aminopropyl triethoxysilane (APTES), FPBA, and sodium cyanoborohydride sequentially to modify boronic acid groups. Then they were incubated in the HRP solution, which could bind with the modified boronic acid groups under alkaline condition. The solution was replaced by APBA solution subsequently, contributing to the covalent bond of APBA and the HRP on the inner surface of the SCCBs. After that, the pregel solution was used to fill the voids of the SCCBs. With the ultraviolet (UV) light, the solution in and out of the SCCBs was polymerized, and the sandwich-like SCCB/HRP/hydrogel hybrid particles were obtained. Finally, HF was employed to remove the SCCBs and HRP templates, with remaining porous hydrogel scaffolds. TMB single-component solution was used to determinate the activity of HRP before and after etching. The colorimetric assay at 450 nm shown in Fig. S2 indicates that there is little residual HRP in the MIP particles. Therefore, the oriented surface imprinted boronate affinity inverse opal MIP particles were prepared after the removal of the SCCBs and HRP templates.

The microstructures of SCCB and oriented boronate affinity–imprinted inverse opal particle were observed by SEM, as shown in Fig. 2. The SCCB was assembled by close packed silica nanoparticles and showed face-center-cubic (FCC) structure both on the surface and inner of the bead (Fig. 2b, c). Besides, the SCCBs showed good monodispersity (Fig. S3). With the large specific surface area and connected nanochannels of the microstructure, the SCCB is superb in the aspects of sufficient HRP immobilization sites and convenient hydrogel filling channels (Fig. 2d). After the removal of silica templates and immobilized HRP, the polymerized hydrogel scaffold was left. As the hydrogel scaffold is negatively replicated from the SCCB, it inherits the ordered arrangement and exhibits the inverse opal structure. As the hydrogel lack in enough strength, the inverse opal structure with higher concentration of cross-linker was employed and characterized by SEM (Fig. 2e, f). This structure not only exhibits the large

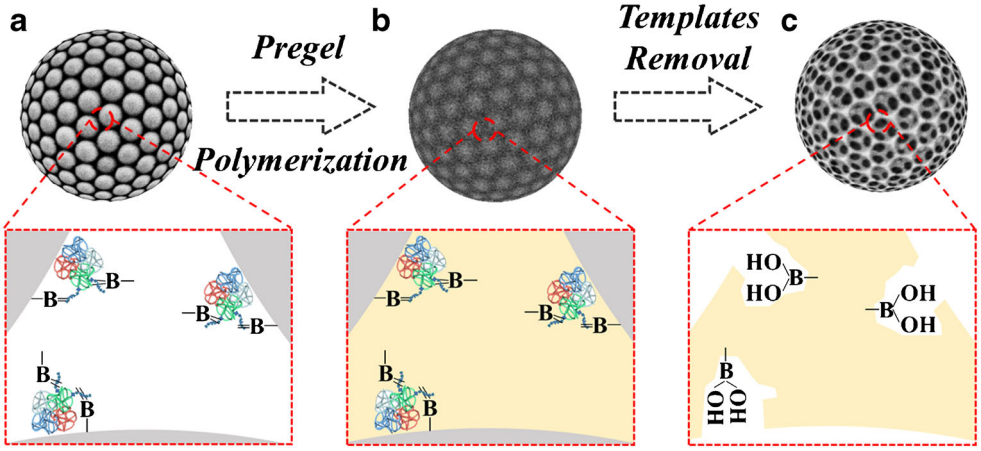


**Fig. 1** Schematic diagram of the preparation process of the oriented surface boronate affinity–imprinted inverse opal particles

specific surface area for imprinting sites but also offers macropores as easier accesses for mass transfer.

In this research, the modification of boronic acid groups of the SCCBs is critical for the preparation of MIP. Therefore, the assay of the modified boronic acid groups on the SCCBs is necessary. Here, we evaluated the modification of boronic acid groups by quantizing the captured HRP on the SCCB based on the specific adsorption of HRP and boronic acid groups. We compared the HRP adsorption abilities of unmodified, amino-modified, and boronic acid modified SCCBs, as shown in Fig. 3a. This controlled experiment is based on two theories. Firstly, the unmodified and amino-modified SCCBs lack the capability of bonding with glycoproteins except non-specific adsorption. In addition, HRP is a kind of efficient enzyme with glycosylation sites and can catalyze TMB to show significant colorimetric reaction. Thus, the unmodified and amino-modified SCCBs exhibited little HRP activity, while the boronic acid modified SCCBs demonstrated a high HRP activity, as shown in Fig. 3a. The result indicates that the SCCBs were modified by the boronic acid groups successfully, and the SCCBs can show excellent capability on binding glycoproteins. The covalent reaction between the boronic acid groups and glycoproteins is revisable and pH-dependent. Thus, the pH of the reaction environment is another influence factor for the specific adsorption of HRP and boronic acid groups. To investigate the impact of pH, we dissolved the HRP in different pH buffer to incubate boronic acid modified SCCBs. The relative bonded amount of the covalent reaction can also be estimated by the TMB colorimetric reaction. As the results shown in Fig. 3b, the binding of HRP was negative affected by the acidic environment significantly, and it reached a plateau when the solution was alkalescent. Thus, to obtain the best performance of imprinting, the whole preparation process of the MIP should be under alkaline condition.

To fabricate the inverse opal particles, *N,N′*-methylenebis(acrylamide) (Bis) and acrylamide (AAm) are employed as the monomer and cross-linker of the pregel, respectively. The polymerization is initiated by the photoinitiator with UV light. As the time of polymerization process is very short, it had tiny influence on the activity of HRP (Fig. S4). It is worth mentioning that the ratio and concentration of AAm and Bis also have effect on the resultant MIP particles. Both of the higher ratio of AAm to Bis and lower concentration of pregel solution would result in the

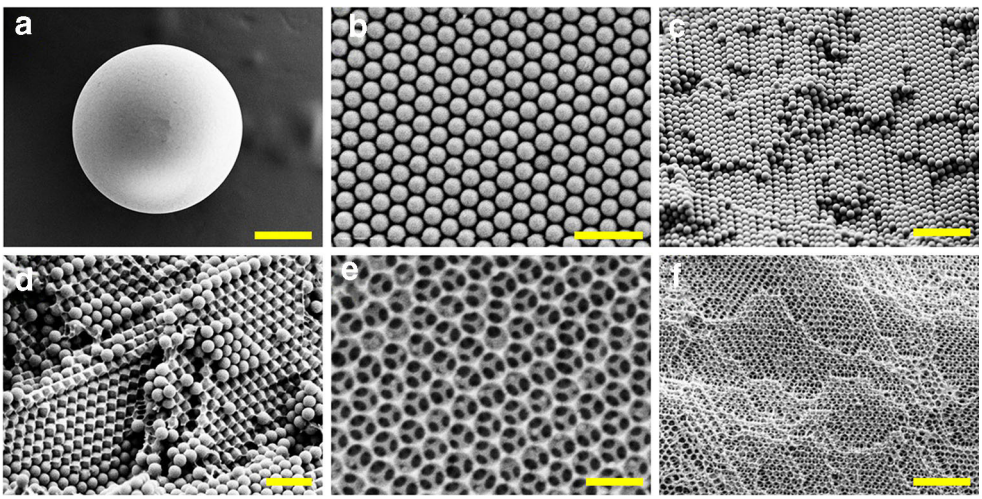


**Fig. 2** SEM characterization. **a**) A whole SCCB; **b**, **c** the microstructure of the surface and the inside of a SCCB; **d** the microstructure of the inside of a hybrid particle; and **e**, **f** the microstructure of the surface and the inside of an inverse opal particle. The bars are 100 μm in (**a**), 1 μm in (**b** and **d**), 2 μm in (**c** and **f**), and 500 nm in (**e**)

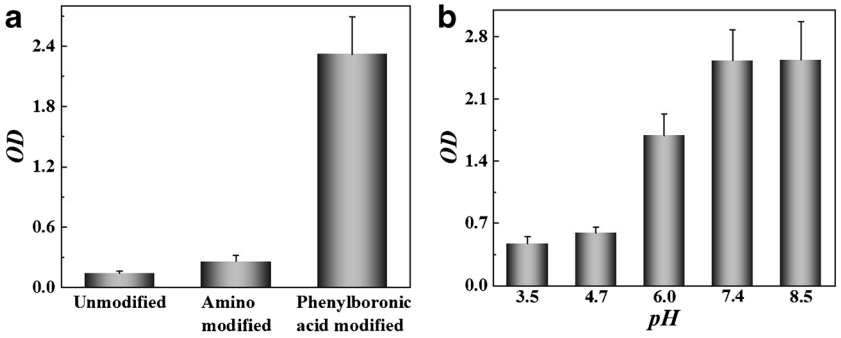


**Fig. 3** The conditions optimization of the preparation process. **a** The effect of the pre-modification of the SCCBs and **b** the effect of the pH of the HRP solution. The number of replicates was five. Error bars represent standard deviations

lower mechanical strength of the inverse opal particles. These bring the disadvantages of imprinting site damage and non-specific adsorption. Therefore, considering the above reasons, the pregel solution with the concentration of 20 wt%, and a ratio of 29:1 (AAm to Bis) was chosen.

To demonstrate the capability of the oriented imprinted inverse opal particles for glycoprotein assay, we prepared HRP-oriented imprinted inverse opal MIP particles under the optimized conditions (Fig. 4a–c). The non-molecularly imprinted polymer (NIP) particles were prepared by the same procedures without HRP. When the MIP particles were incubated in HRP solution, HRP molecules accessed to the complementary imprinting sites on the hydrogel scaffold and bind with them closely based on the boronate affinity. Meanwhile, the NIP particles only exhibited little nonspecific adsorption (Fig. 4d, e). The imprinting factor value of this type of MIP particles is 16.03. This suggests that the MIP particles can be used as artificial probe for the template molecules. To further study the specificity of the MIP for the target recognition, the HRP-imprinted particles were examined by HRP solutions with high concentration impurities. Small molecules of saccharides (e.g., glucose, mannose, and galactose), non-glycoproteins (e.g., BSA and ribonuclease A), and other type of glycoproteins (e.g., TRF, ribonuclease B and alkaline phosphatase) are potential interferences. Thus, the MIP particles were used to assay the HRP in the solution with high concentration of glucose, BSA, or TRF, respectively. Figure 5a displays the colorimetric reaction results of the MIP particles after being incubated in these solutions. It is obvious that the MIP particles still had the capability for recognizing the target molecules even though there were different types of interfering agents with thousands-fold higher concentration. The reduced binding can be attributed to the steric effect of the high concentration interfering reagents and competitive binding (glucose). The effect of incubation time is also discussed, as shown in Fig. 5b. It is found that the binding amount of MIP particles were increasing along the time and reached equilibrium in less than 2 h, which can be ascribed to the microstructure of the particles. This mass transfer efficiency in the MIP particles is acceptable; thus, the MIP particles are applicable to be used for assay.

On account of the covalent binding between boronic acid groups and glycoproteins is pH-dependent, the pH of the test solution was also investigated. A series of HRP solutions with different pH were prepared to incubate the MIP particles for this purpose. As expected, the NIP particles showed little capability on binding with HRP under different pH conditions, while the MIP particles showed great capability of binding

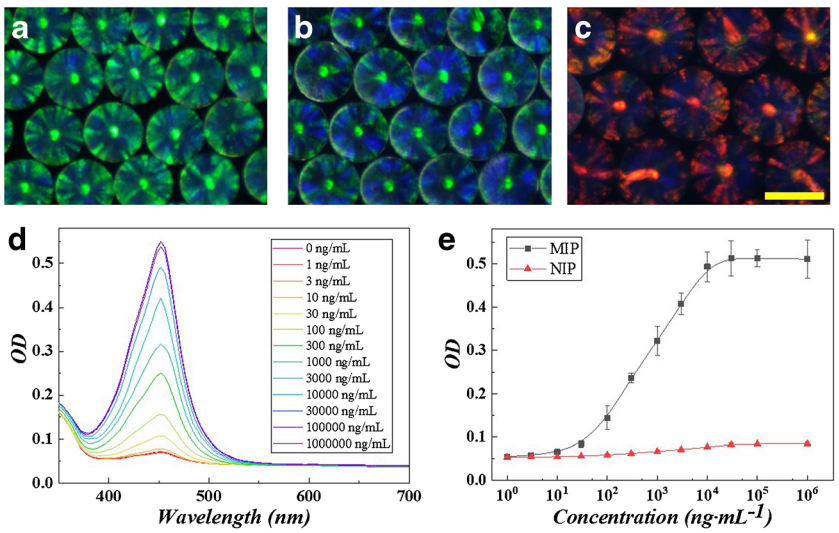


**Fig. 4** Optical images characterization and concentration curve. **a**-**c** The optical images of SCCBs, hybrid particles, and inverse opal particles; **d** the HRP activities of the MIP particles incubated in different concentrations of the target HRP; **e** the HRP activities of MIP and NIP particles incubated in different concentrations of the target HRP. The bar is 300 μm in (**a**–**c**). The number of replicates was five in (**e**), and error bars represent standard deviations

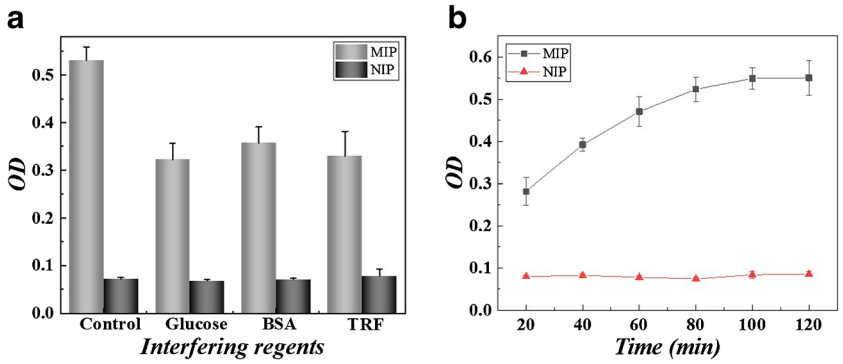


**Fig. 5** The specificity and incubation time of the oriented MIP particles. **a** The specificity of the oriented MIP particles and **b** the optimization of the incubation time of the oriented MIP particles. The number of replicates was five. Error bars represent standard deviations

HRP and positive correlation with the pH of the solution (Fig. S5). This indicates that there were phenylboronic acid molecules existed on the MIP particles, and the pH sensitive reaction was carried out. It is worth noting that most samples from human were at the range of 5.0 to 8.5; thus, the MIP particles can be applied for the real sample applications.

To investigate more practical applications of the oriented surface MIP particles, we fabricated AFP-imprinted particles with the similar approach for the AFP analysis. AFP is a kind of glycoprotein with 11 glycosylation sites and has been widely used as tumor marker in the clinical screening of various cancers, especially the liver cancer. We used AFP-imprinted particles to bind with AFP in the sample solution and then incubated them with HRP-tagged anti-AFP. The particles that bind with AFP successfully were tagged with HRP by this sandwich ELISA method, which were then demonstrated by the colorimetric reaction (Fig. S6). The results show that the AFP-imprinted MIP particles had a good linearity to the standard AFP solution with low concentrations (1–50 ng $mL^{-1}$), and the limit of detection (LOD) is 1.32 ng $mL^{-1}$.We compared the strategy we presented with some kinds of recently reported nanomaterial-based optical methods, as shown in Table 1 [37–41]. Electrochemical aptasensor method can provide a very low LOD. Nevertheless, the complicated modifications of the electrode and poor selectivity ability restrict its wide application, while the label-free MIP particles can recognize glycoprotein with high selectivity. This indicates that the MIP particles have great potential of AFP quantitative analysis in practical applications. The AFP-imprinted MIP particles also were used directly for the binding of HRP, and the result is shown in Fig. S7. The result indicates that the AFP-imprinted MIP particles only have similar nonspecific adsorption as NIP particles. Hence, the MIP particles perform a high degree of selectivity for the imprinted glycoprotein and a low level of nonspecific adsorption. Typically, we assayed the AFP in human serum using our AFP-imprinted particles. The calculated concentration of AFP is about 7.30 ng $mL^{-1}$ according to Fig. S6b and 9.95 ng $mL^{-1}$ by standard addition method shown in Fig. 6, which is consistent with the value quantized by AFP kit (8.52 ng $mL^{-1}$).

It is noting that this strategy uses the glycoprotein with at least 2 glycosylation sites as the template. Hence, some kinds of glycoprotein with only 1 glycosylation site (e.g., ribonuclease B) cannot be involved in this method. In addition, the binding between the boronate and glycoprotein realizes in weak alkaline solution; therefore, the MIP particles are inapplicable for the determination of glycoprotein in acidic solution.

**Table 1** An overview on recently reported nanomaterial-based optical methods for the determination of glycoproteins

| Materials | Detection method | Linear range | LOD | References |
|---|---|---|---|---|
| MIP film | Immunochemiluminescence assay | – | 1 ng $mL^{-1}$ | [7] |
| Gold nanocluster-molybdenum disulfide | Fluorescence aptasensor | 0.5–60 ng $mL^{-1}$ | 0.16 ng $mL^{-1}$ | [37] |
| 5-Carboxyfluorescein-labeled AFP aptamer and palladium nanoparticles | Fluorescence aptasensor | 5.0–150 ng $mL^{-1}$ | 1.38 ng $mL^{-1}$ | [38] |
| Zinc sulfide-cadmium telluride hierarchical porous nanospheres | Colorimetric detection<br>Fluorometric detection | 0.04–64 ng $mL^{-1}$<br>0.05–12 ng $mL^{-1}$ | 0.01 ng $mL^{-1}$<br>0.007 ng $mL^{-1}$ | [39] |
| Mixed self-assembled aptamers and zwitterionic peptides | Electrochemical aptasensor | 10.0 fg $mL^{-1}$ −100.0 pg $mL^{-1}$ | 3.1 fg $mL^{-1}$ | [40] |
| dsDNA and methyl violet | Resonance light scattering aptasensor | 5–100 ng $mL^{-1}$ | 0.94 ng $mL^{-1}$ | [41] |
| MIP particles | Colorimetric detection | 1–50 ng $mL^{-1}$ | 1.32 ng $mL^{-1}$ | This work |

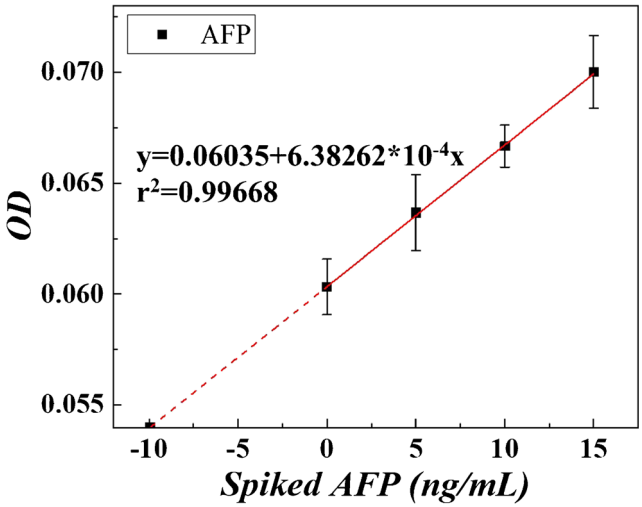


**Fig. 6** The practical application the oriented MIP particles. The oriented MIP particles were incubated in the human serum. The number of replicates was five. Error bars represent standard deviations

## Conclusion

In conclusion, we presented a novel kind of oriented surface boronate affinity inverse opal particles as biomimetic antibody particles and demonstrated their potential in target glycoprotein assay. Because of their microstructure, the particles gave large surface specific area and many oriented surface imprinting sites of target glycoprotein. As there are no boronic acid groups out of the imprinting sites, the particles are endowed with higher specificity. The modification of SCCBs and the pH of the glycoprotein solution were also discussed and optimized. When the particles were used for determination, they exhibited favorable sensitivity, specificity, and potential in clinical screening. These features of the oriented surface boronate affinity inverse opal particles indicate that they can play a key role in the future for medical diagnosis and the study of glycoproteins.

**Acknowledgments** The authors thank Yuanjin Zhao for the scientific discussion.

**Data and materials availability** All data needed to evaluate the conclusions in the paper are present in the paper and/or the Supplementary Materials. Additional data related to this paper may be requested from the authors.

**Author contributions** H. Wang and J. Wang contributed equally. T. Kong designed research; H. Wang, J. Wang, and X. Wang performed research; H. Wang and J. Wang analyzed data and wrote the paper; Y. Wang, Y. Liu, R. Liu, H. Tan, and T. Wang contributed to scientific discussion of the article.

**Funding information** This work was supported by the National Natural Science Foundation of China (Grant Nos. 61927805 and 51522302); the NSAF Foundation of China (Grant No. U1530260); the Natural Science Foundation of Jiangsu Province (Grant No. BE2018707); the Postdoctoral Science Foundation of China (Grant No. 2019 M653061); the Guangdong Basic and Applied Basic Research Foundation (2019A1515111155); the Natural Science Foundation of Guangdong Province (2019A1515011750); Science, Technology, and Innovation Commission of Shenzhen Municipality (JCYJ20170817171930009, JCYJ20180507183036060; JCYJ20190808120405672); the Guangdong Innovation Platform of Translational Research for Cerebrovascular Diseases; and the Scientific Research Foundation of Southeast University.

## Compliance with ethical standards

**Conflict of interest** The authors declare that they have no competing of interests.

## References

1. Cohen L, Walt DR (2019) Highly sensitive and multiplexed protein measurements. Chem Rev 119:293–321
2. Lawal AT (2018) Progress in utilisation of graphene for electrochemical biosensors. Biosens Bioelectron 106:149–178
3. Zong C, Xu M, Xu L, Wei T, Ma X, Zheng X, Hu R, Ren B (2018) Surface-enhanced raman spectroscopy for bioanalysis: reliability and challenges. Chem Rev 118:4946–4980
4. Xu Y, Wang H, Chen B, Liu H, Zhao Y (2019) Emerging barcode particles for multiplex bioassays. Sci China Mater 62:289–324
5. Yuan H, Chao Y, Li S, Tang MYH, Huang Y, Che Y, Wong AST, Zhang T, Shum H (2018) Picoinjection-enabled multitarget loop-mediated isothermal amplification for detection of foodborne pathogens. Anal Chem 90:13173–13177
6. Luan C, Xu Y, Fu F, Wang H, Xu Q, Chen B, Zhao Y (2017) Responsive photonic barcodes for sensitive multiplex bioassay. Nanoscale 9:14111–14117
7. Li L, Lu Y, Bie Z, Chen H, Liu Z (2013) Photolithographic boronate affinity molecular imprinting: a general and facile approach for glycoprotein imprinting. Angew Chem Int Ed 52:7451–7454
8. Wang H, Xu Q, Shang L, Wang J, Rong F, Gu Z, Zhao Y (2016) Boronate affinity molecularly imprinted inverse opal particles for multiple label-free bioassays. Chem Commun 52:3296–3299
9. Pan X, He X, Liu Z (2018) Molecularly imprinted mesoporous silica nanoparticles for specific extraction and efficient identification of Amadori compounds. Anal Chim Acta 1019:65–73
10. Zhang X, Cui Y, Bai J, Sun Z, Ning B, Li S, Wang J, Peng Y, Gao Z (2017) Novel biomimic crystalline colloidal array for fast detection of trace parathion. ACS Sens 2:1013–1019
11. Mori K, Hirase M, Morishige T, Takano E, Sunayama H, Kitayama Y, Inubushi S, Sasaki R, Yashiro M, Takeuchi T (2019) A pretreatment-free, polymer-based platform prepared by molecular imprinting and post-imprinting modifications for sensing intact exosomes. Angew Chem Int Ed 58:1612–1615
12. Hu X, An Q, Li G, Tao S, Liu J (2006) Imprinted photonic polymers for chiral recognition. Angew Chem Int Ed 45:8145–8148
13. Liu Z, Balasubramanian V, Bhat C, Mahermo V, Mäkilä E, Kemell M, Fontana F, Janoniene A, Petrikaite V, Salonen J, Yli-Kauhaluoma J, Hirvonen J, Zhang H, Santos HA (2017) Quercetin-based modified porous silicon nanoparticles for enhanced inhibition of doxorubicin-resistant cancer cells. Adv Healthc Mater 6:1601009
14. Schirhagl R (2014) Bioapplications for molecularly imprinted polymers. Anal Chem 86:250–261
15. Badugu R, Lakowicz JR, Geddes CD (2004) Noninvasive continuous monitoring of physiological glucose using a monosaccharide-sensing contact lens. Anal Chem 76:610–618

16. Ramsay WJ, Bayley H (2018) Single-molecule determination of the isomers of d-glucose and d-fructose that bind to boronic acids. Angew Chem Int Ed 57:2841–2845
17. Liu H, Li Y, Sun K, Fan J, Zhang P, Meng J, Wang S, Jiang L (2013) Dual-responsive surfaces modified with phenylboronic acid-containing polymer brush to reversibly capture and release cancer cells. J Am Chem Soc 135:7603–7609
18. Pan X, Chen Y, Zhao P, Li D, Liu Z (2015) Highly efficient solid-phase labeling of saccharides within boronic acid functionalized mesoporous silica nanoparticles. Angew Chem Int Ed 54:6173–6176
19. Xing R, Wang S, Bie Z, He H, Liu Z (2017) Preparation of molecularly imprinted polymers specific to glycoproteins, glycans and monosaccharides via boronate affinity controllable-oriented surface imprinting. Nat Protoc 12:964–987
20. Bie Z, Chen Y, Ye J, Wang S, Liu Z (2015) Boronate-affinity glycan-oriented surface imprinting: a new strategy to mimic lectins for the recognition of an intact glycoprotein and its characteristic fragments. Angew Chem Int Ed 54:10211–10215
21. Fu F, Chen Z, Zhao Z, Wang H, Shang L, Gu Z, Zhao Y (2017) Bio-inspired self-healing structural color hydrogel. Proc Natl Acad Sci U S A 114:5900–5905
22. Gao N, Tian T, Cui J, Zhang W, Yin X, Wang S, Ji J, Li G (2017) Efficient construction of well-defined multicompartment porous systems in a modular and chemically orthogonal fashion. Angew Chem Int Ed 56:3880–3885
23. Wang D, Salgueiriño-Maceira V, Liz-Marzán LM, Caruso F (2002) Gold-silica inverse opals by colloidal crystal templating. Adv Mater 14:908–912
24. Yang B, Li L, Du K, Fan B, Long Y, Song K (2018) Photo-responsive photonic crystals for broad wavelength shifts. Chem Commun 54:3057–3060
25. Lee HG, Jeon TY, Lee SY, Lee SY, Kim SH (2018) Designing multicolor micropatterns of inverse opals with photonic bandgap and surface plasmon resonance. Adv Funct Mater 28:1706664
26. Zhu B, Fu Q, Chen K, Ge J (2018) Liquid photonic crystals for mesopore detection. Angew Chem Int Ed 57:252–256
27. Zhong K, Li J, Liu L, Van Cleuvenbergen S, Song K, Clays K (2018) Instantaneous, simple, and reversible revealing of invisible patterns encrypted in robust hollow sphere colloidal photonic crystals. Adv Mater 30:1707246
28. Li C, Zhao M, Zhou X, Li H, Wang Y, Hu X, Li M, Shi L, Song Y (2018) Janus structural color from a 2D photonic crystal hybrid with a fabry-perot cavity. Adv Opt Mater 6:1800651
29. Zhang H, Zhu Y, Qu L, Wu H, Kong H, Yang Z, Chen D, Makila E, Salonen JJ, Santos HA, Hai M, Weitz DA (2018) Gold nanorods conjugated porous silicon nanoparticles encapsulated in calcium alginate Dano hydrogels using microemulsion templates. Nano Lett 18:1448–1453
30. Chen G, Yu Y, Wang G, Gu G, Wu X, Ren J, Zhang H, Zhao Y (2018) Microfluidic electrospray vitamin metal-organic frameworks encapsulated microcapsules for wound healing. Research 2019:6175398
31. Zhao C, Yu Y, Wu X, Ren J, Zhao Y (2019) Biomimetic intestinal barrier based on microfluidic encapsulated sucralfate microcapsules. Sci Bull 64:1418–1425
32. Zhang H, Liu Y, Wang J, Shao C, Zhao Y (2019) Tofu-inspired microcarriers from droplet microfluidics for drug delivery. Sci China Chem 62:87–94
33. Choi TM, Park JG, Kim YS, Manoharan VN, Kim SH (2015) Osmotic-pressure-mediated control of structural colors of photonic capsules. Chem Mater 27:1014–1020
34. Hou J, Li M, Song Y (2018) Recent advances in colloidal photonic crystal sensors: materials, structures and analysis methods. Nano Today 22:132–144
35. Ge J, Yin Y (2011) Responsive photonic crystals. Angew Chem Int Ed 50:1492–1522
36. Zhang H, Liu Y, Chen G, Wang H, Chen C, Li M, Lu P, Zhao Y (2020) Immunotherapeutic silk inverse opal particles for post-surgical tumor treatment. Sci Bull 65:380–388
37. Xu S, Feng X, Gao T, Liu G, Mao Y, Lin J, Yu X, Luo X (2017) Aptamer induced multicoloured AuNCs-MoS2 "switch on" fluorescence resonance energy transfer biosensor for dual color simultaneous detection of multiple tumor markers by single wavelength excitation. Anal Chim Acta 983:173–180
38. Li G, Zeng J, Liu H, Ding P, Liang J, Nie X, Zhou Z (2019) A fluorometric aptamer nanoprobe for alpha-fetoprotein by exploiting the FRET between 5-carboxyfluorescein and palladium nanoparticles. Microchim Acta 186:314
39. Zhu D, Hu Y, Zhang X, Yang X, Tang Y (2019) Colorimetric and fluorometric dual-channel detection of α-fetoprotein based on the use of ZnS-CdTe hierarchical porous nanosphere. Microchim Acta 186:124
40. Cui M, Wang Y, Jiao M, Jayachandran S, Wu Y, Fan X, Luo X (2017) Mixed self-assembled aptamer and newly designed zwitterionic peptide as antifouling biosensinginterface for electrochemical detection of alpha-fetoprotein. ACS Sens 2:490–494
41. Chen F, Zhang F, Liu Y, Cai C (2018) Simply and sensitively simultaneous detection hepatocellular carcinoma markers AFP and miRNA-122 by a label-free resonance light scattering sensor. Talanta 186:473–480